

092630

832-210-105

RECEIVED BY

ESA - SDS 3 APR 1984

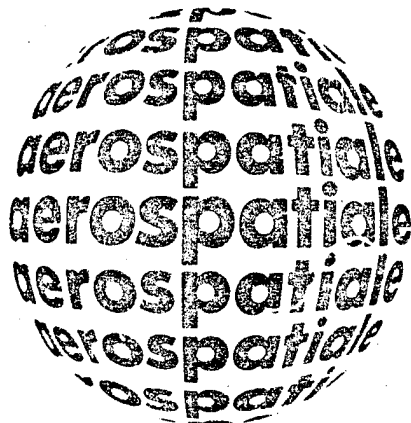
DATE:

DCAS N. 090922

RECEIVED BY

ESA - SDS FACILITY

ESA - SDS FACILITY



DISTRIBUTION STATEMENT A

Approved for public release  
Distribution Unlimited

DTIC QUALITY INSPECTED 4

(SRIAS-832-210-105) A NEW METHOD OF  
ANALYSIS OF COMPOSITE STRUCTURES (Societe  
Nationale Industrielle Aerospatiale) 14 p  
EC A02/AF A01

N84-25773

Unclas

G6/24 92630

19960226 009

DEPARTMENT OF DEFENSE  
NAVAL TECHNICAL EVALUATION CENTER  
WASHINGTON, D. C. 20340

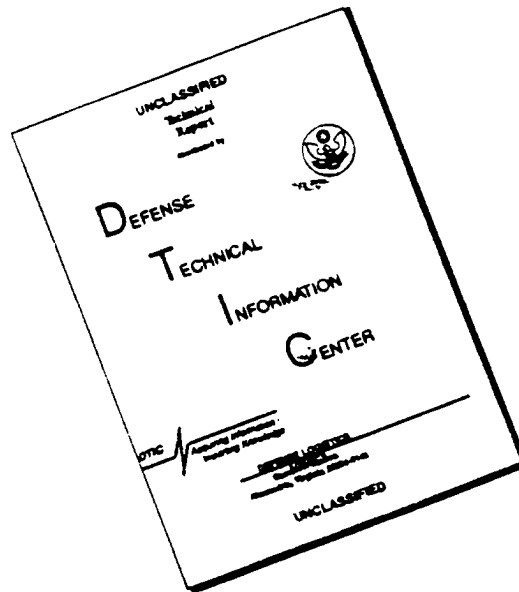
SOCIÉTÉ NATIONALE INDUSTRIELLE

aerospatiale

37, BOULEVARD DE MONTMORENCY, 75781 PARIS CEDEX 16 - TEL. : 524-43-21

19960226 009

# DISCLAIMER NOTICE



THIS DOCUMENT IS BEST QUALITY AVAILABLE. THE COPY FURNISHED TO DTIC CONTAINED A SIGNIFICANT NUMBER OF PAGES WHICH DO NOT REPRODUCE LEGIBLY.

**NINTH EUROPEAN ROTORCRAFT AND POWERED LIFT AIRCRAFT FORUM**

**Paper No. 88**

**A NEW METHOD OF ANALYSIS  
OF COMPOSITE STRUCTURES**

**G. DUVAUT**

Université Pierre et Marie Curie  
4 Place Jussieu - 75005 PARIS

**M. NUC**

Société Nationale Industrielle Aérospatiale  
Helicopter Division  
Marignane, France

**September 13 - 14 - 15, 1983**

**Stresa, Italy**

**EUROPEAN ROTORCRAFT FORUM C/O AGUSTA, CP 480 GALLARATE (VA), ITALY**

# A NEW METHOD OF ANALYSIS OF COMPOSITE STRUCTURES

G. DUVAUT

INRIA, Domaine de Voluceau - 78153 LE CHESNAY Cedex  
and Université Pierre et Marie Curie, 4 Place Jussieu - 75005 PARIS

M. NUC

AEROSPATIALE, MARIGNANE - 13725 MARIGNANE Cedex

## 1 - INTRODUCTION

Composite materials consisting of high tensile resin-impregnated fibers are being more and more frequently used in structures capable of high mechanical performance. Direct calculation of deformation of these structures using the finite elements method raises major difficulties due mainly to the very high number of heterogeneities in the material. Computation methods are, therefore, based on investigation of equivalent homogeneous materials, i.e. effective behavior moduli (Willis, Hashin ...).

In this paper we use the homogenization method. This method applies when the material being investigated has a periodic structure. It can then be shown that when the dimensions of the period tend homothetically to zero the fields of deformation and stresses tend to those corresponding to a homogeneous structure whose elastic properties can be computed precisely when a single period of the composite medium to be investigated is known. This boundary value structure is the homogenized structure and its behavior coefficients are the homogenized coefficients. This is the macroscopic equivalent structure. Furthermore by a localization procedure the method allows an easy computation of the microscopic field of stresses and, in particular, of stress forces at the boundaries between fibers and matrix. These stress forces are particularly important because they can initiate cracks and delaminations. The overstresses at the microscopic level may produce fiber ruptures.

After presenting the general method of homogenization, which leads first to an homogenized equivalent macroscopic structure and secondly to a localization procedure for computing the field of microscopic stresses and stress forces, we apply the method to two types of composite materials :

- i) Material reinforced by periodically arranged, parallel fibers (Figure 1)

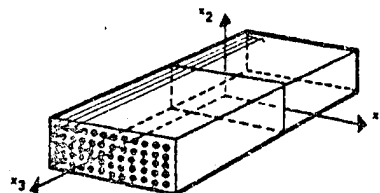


Fig. 1 : PARALLEL FIBERS

- ii) Material consisting of a very large number of parallel layers of homogeneous materials superposed periodically (Figure 2)

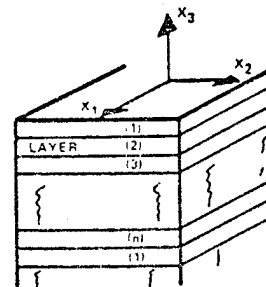


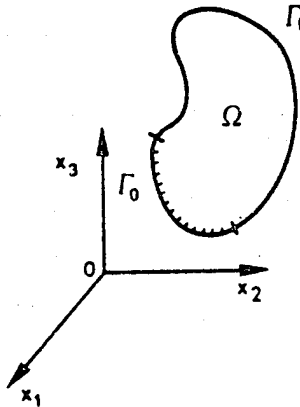
Fig. 2 : MULTIPLE LAYERS

This is followed by the numerical results obtained by using the MODULEF code.

## 2 - DESCRIPTION OF THE HOMOGENIZATION METHOD [1] [4] [5] [10] [12]

### 2.1 - Formulation of the problem

Let us consider an elastic body which occupies a region  $\Omega$  related to a system of orthonormal axes  $Ox_1 x_2 x_3$ . This body is subjected to a system of voluminal forces  $\{f_i\}$  and surface forces  $\{F_i\}$  on a portion  $\Gamma_F$  of boundary  $\partial\Omega$ . The other portion of the boundary is  $\Gamma_0$ , to which a zero movement condition is imposed.



The field of stresses at equilibrium satisfies the equilibrium equations

$$1) \frac{\delta \sigma_{ij}}{\delta x_j} + f_i = 0 \quad \text{in } \Omega$$

$$2) \sigma_{ij} n_j = F_i \quad \text{on } \Gamma_F.$$

Furthermore, the material is elastic with fine periodic structure, i.e.  $\Omega$  is covered by a set of identical periods of rectangular (Fig. 4) or hexagonal (Fig. 5) or more complicated shape such as the examples

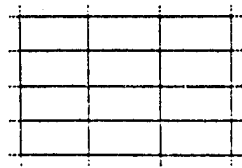


Fig. 4 : MATERIALS WITH FINE PERIODIC STRUCTURE

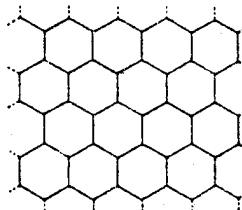


Fig. 5 : MATERIALS WITH FINE PERIODIC STRUCTURE

given in Figures 6 and 7.

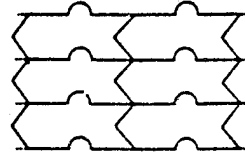


Fig. 6 : MATERIALS WITH FINE PERIODIC STRUCTURE

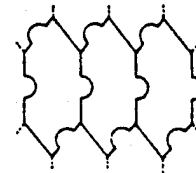


Fig. 7 : MATERIALS WITH FINE PERIODIC STRUCTURE

All the period forms must be such that opposing faces which correspond in a translation can be defined two by two.

In all cases we shall designate as  $Y$  a period characteristic of the material which has been enlarged by homothetics and fixed once and for all.  $\epsilon$  then designates the homothetic ratio which is small and which takes us from  $Y$  to a period in the elastic material. The elastic structure of the material is then fully known if it is given over a single period, e.g. the enlarged period  $Y$  related to the orthonormal axis system  $Oy_1 y_2 y_3$ . Then let  $a_{ijkh}(y)$  be the coefficients of elasticity on  $Y$ , which generally alter very quickly with respect to  $y$ , but satisfy in all respects the symmetry relation

$$a_{ijkh}(y) = a_{jikh}(y) = a_{khij}(y)$$

and positivity relation

$$\exists \alpha_0 > 0, a_{ijkh}(y) \tau_{ij} \tau_{kh} \geq \alpha_0 \tau_{ij} \tau_{ij}, \forall \tau_{ij} = \tau_{ji}$$

The functions  $y \rightarrow a_{ijkh}(y)$  defined on  $Y$  are extended by  $Y$ -periodicity to the entire space  $Oy_1 y_2 y_3$  assumed to be covered by contiguous periods identical to  $Y$ .

The coefficients of elasticity in the material  $\Omega$  are then  $a_{ijkh}^\epsilon(x)$  defined by :

$$a_{ijkh}^\epsilon(x) = a_{ijkh}(y), \quad y = \frac{x}{\epsilon}$$

For greater simplification in the text we shall write :

$$a(y) = \{a_{ijkh}(y)\}, \quad a^\epsilon(x) = a\left(\frac{x}{\epsilon}\right), \quad \sigma = \{\sigma_{ij}\}$$

and shall consider  $a(y)$  or  $a^\epsilon(x)$  as known matrix  $6 \times 6$  indexed by the symmetrical pairs  $(i, j)$ .

The law of elasticity

$$3) \sigma_{ij} = a_{ijkh} \epsilon(x) e_{kh}(u)$$

is written

$$\sigma = a^\epsilon(x) e(u),$$

where

$$e(u) = \{e_{ij}(u)\}, \quad e_{ij}(u) = \frac{1}{2} \left( \frac{\delta u_i}{\delta x_j} + \frac{\delta u_j}{\delta x_i} \right)$$

When an ambiguity is possible, either  $e_x(u)$  or  $e_y(u)$  will be specified depending on whether the drift occurs with respect to  $x$  or  $y$ . The boundary conditions are finalized by

$$4) u = 0 \text{ on } \Gamma_0$$

The problem posed by (1) (2) (3) (4) has a unique solution which depends on  $\epsilon$  and which we shall designate  $u^\epsilon$ ; to this corresponds a field of stresses  $\sigma^\epsilon$  given by :

$$5) \sigma^\epsilon = a^\epsilon(x) e(u^\epsilon)$$

Numerically it is very difficult when  $\epsilon$  is small to calculate  $u^\epsilon$  since there are a large number of heterogeneities in the elastic medium. We therefore try to obtain a limited expansion of the solution  $u^\epsilon, \sigma^\epsilon$ .

## 2.2 - Asymptotic expansions

The solution is affected by two factors :

- i) The first is the scale of  $\Omega$  and arises from the forces applied and the conditions at the boundaries.
- ii) The second is due to the periodic structure ; it is on the same scale as the period and is repeated periodically.

This justifies looking for an asymptotic expansion of the form :

$$6) u^\epsilon = u^0(x, y) + \epsilon u^1(x, y) + \epsilon^2 u^2(x, y) + \dots$$

where the  $u^\alpha(x, y)$  are, for each  $x \in \Omega$ ,  $Y$ -periodic functions with respect to the variable  $y \in Y$ . Then  $y = \frac{x}{\epsilon}$  is applied to (6). Associated with the expansion (6) is an expansion of the field of deformation  $e(u^\epsilon)$  (\*).

$$7) e(u^\epsilon) = \frac{1}{\epsilon} e_y(u^0) + e_x(u^0) + e_y(u^1) + \epsilon [e_x(u^1) + e_y(u^2)] + \dots$$

and of the field of stresses  $\sigma^\epsilon$

$$8) \sigma^\epsilon = \frac{1}{\epsilon} \sigma^0(x, y) + \sigma^1(x, y) + \epsilon \sigma^2(x, y) + \dots$$

with

$$\begin{aligned} \sigma^0(x, y) &= a(y) e_y(u^0) \\ \sigma^1(x, y) &= a(y) [e_y(u^1) + e_x(u^0)] \\ \sigma^2(x, y) &= a(y) [e_y(u^2) + e_x(u^1)] \end{aligned}$$

The equilibrium equations (1) applied to  $\sigma^\epsilon$  give

$$\frac{\delta}{\delta x_j} \sigma^\epsilon_{ij} + f_i = 0$$

or in a more condensed form

$$9) \operatorname{div} \sigma^\epsilon + f = 0.$$

Given the expansion (8) of  $\sigma^\epsilon$  we have (\*\*)

$$\begin{aligned} 10) \frac{1}{\epsilon^2} \operatorname{div}_y \sigma^0 + \frac{1}{\epsilon} (\operatorname{div}_y \sigma^1 + \operatorname{div}_x \sigma^0) \\ + \operatorname{div}_y \sigma^2 + \operatorname{div}_x \sigma^1 + f + \dots = 0. \\ x \in \Omega, y \in Y. \end{aligned}$$

The boundary conditions (2) are treated in the same way :

$$11) \frac{1}{\epsilon} \sigma^0 \cdot n + \sigma^1 \cdot n - F + \epsilon \sigma^2 \cdot n + \dots = 0 \\ \text{for } x \in \Gamma_F, y \in Y.$$

Finally the conditions (4) mean that

$$12) u^0 + \epsilon u^1 + \epsilon^2 u^2 + \dots = 0 \\ \text{for } x \in \Gamma_0, y \in Y.$$

By making the various powers of  $\epsilon$  zero we obtain :

$$\begin{aligned} 13) \begin{cases} \operatorname{div}_y \sigma^0 = 0 \\ \sigma^0 = a(y) e_y(u^0) \end{cases} \\ 14) \begin{cases} \operatorname{div}_y \sigma^1 + \operatorname{div}_x \sigma^0 = 0 \\ \sigma^1 = a(y) [e_y(u^1) + e_x(u^0)] \end{cases} \\ 15) \begin{cases} \operatorname{div}_y \sigma^2 + \operatorname{div}_x \sigma^1 + f = 0 \\ \sigma^2 = a(y) [e_y(u^2) + e_x(u^1)] \end{cases} \end{aligned}$$

The equations (11) and (12) will be used later.

(\*) Note that

$$\frac{d}{dx_i} u^\alpha(x, y) = \frac{\delta}{\delta x_i} u^\alpha(x, y) + \frac{1}{\epsilon} \frac{\delta}{\delta y_i} u^\alpha(x, y)$$

$$(**) \operatorname{div}_y \sigma^\alpha = \left\{ \frac{\delta \sigma^\alpha_{ij}}{\delta y_j} \right\}; \operatorname{div}_x \sigma^\alpha = \left\{ \frac{\delta \sigma^\alpha_{ij}}{\delta x_j} \right\}$$

### 2.3 - Resolutions

The systems (13) (14) (15) contain differential operators in  $y$ . They therefore constitute equations with partial derivatives on the period of base  $Y$ , the unknown factors being the  $Y$ -periodic functions.

**System (13) :** This leads immediately to :

$$16) \sigma^0 = 0, u^0 = u^0(x)$$

**System (14) :** In view of (16) it is reduced to :

$$17) \operatorname{div}_y \sigma^1 = 0, \sigma^1 = a(y) [e_y(u^1) + e_x(u^0)]$$

The deformation  $e_x(u^0)$  is a function only of  $x$ ; it therefore plays the role of a parameter with respect to the differential system in  $y$ . Due to the linearity,  $\sigma^1, u^1$  may therefore be written in the form :

$$18) \begin{cases} \sigma^1 = s^{kh}(y) e_{kh}(u^0) \\ u^1 = \chi^{kh}(y) e_{kh}(u^0) \end{cases}$$

where

$$e_{kh}(u^0) = \frac{1}{2} \left( \frac{\delta u^0_k}{\delta x_h} + \frac{\delta u^0_h}{\delta x_k} \right)$$

$$19) \begin{cases} \operatorname{div}_y s^{kh} = 0 \\ s^{kh} = a(y) [\sigma^{kh} + e_y(\chi^{kh})] \\ \chi^{kh} \text{ is } Y\text{-periodic} \end{cases}$$

The tensor  $\sigma^{kh}$  has components given by

$$\sigma_{ij}^{kh} = \frac{1}{2} (\delta_{ik} \delta_{jh} + \delta_{ih} \delta_{jk})$$

It can be proved that the system (19) determines the vector  $\chi^{kh}(y)$  to within an additive constant.

For any function  $\Phi = \Phi(x, y)$ , we define

$$\langle \Phi \rangle = \frac{1}{\operatorname{mes} Y} \int_Y \Phi(x, y) dy$$

The solution  $\sigma^1$  of (14) is given by,

$$20) \sigma^1(x, y) = a(y) [\sigma^{kh} - e_y(\chi^{kh})] e_{kh}(u^0),$$

and taking the mean value, we obtain,

$$21) \langle \sigma_{ij}^1 \rangle = q_{ij}^{kh} e_{kh}(u^0)$$

where

$$22) q_{ij}^{kh} = \langle a_{ijkh}(y) \rangle - \langle a_{ijpq}(y) e_{pq}(\chi^{kh}(y)) \rangle$$

**System (15) :** It suffices to take the mean on  $Y$  in the first equation to obtain

$$23) \operatorname{div}_x \langle \sigma^1 \rangle + f = 0 \quad \text{in } \Omega$$

If we introduce  $\Sigma = \langle \sigma^1 \rangle$ , we have

$$24) \begin{cases} \operatorname{div}_x \Sigma + f = 0 & \text{in } \Omega \\ \Sigma_{ij} = q_{ij}^{kh} e_{kh}(u^0) \end{cases}$$

Using equation (12) and taking the mean on  $Y$  in (11), we obtain :

$$25) \begin{cases} u^0 = 0 & \text{on } \Gamma_0 \\ \Sigma_{,n} = F & \text{on } \Gamma_F \end{cases}$$

The system (24) with boundary conditions (25) is a well posed elasticity problem ; the equilibrium equations are unchanged, as well as the boundary conditions. The elastic constitutive relation is

$$\Sigma_{ij} = q_{ij}^{kh} e_{kh}(u^0)$$

It is homogeneous since the coefficients  $q_{ij}^{kh}$  given by (22) are independent of  $x \in \Omega$ . These coefficients define the equivalent homogeneous material. They are called homogenized coefficients. The stress field  $\Sigma = (\Sigma_{ij})$  is called the macroscopic stress field and is defined by

$$\Sigma = \langle \sigma^1 \rangle$$

The strain field  $E = e_x(u^0)$  is called the macroscopic strain field and satisfies

$$E = \langle e_x(u^0) + e_y(u^1) \rangle$$

It can be proved that the homogenized coefficients  $q_{ij}^{kh}$  satisfy

$$\begin{cases} q_{ij}^{kh} = q_{ij}^{kh} (= q_{ijkh}) \\ 3\alpha_1 > 0, q_{ij}^{kh} s_{ij} s_{kh} \geq \alpha_1 s_{ij} s_{ij}, \forall s_{ij} = s_{ji} \end{cases}$$

This shows that  $(q_{ij}^{kh})$  are reasonable elastic coefficients and that the macroscopic scale problem (24) (25) has a unique solution.

### 2.3 - Microscopic fields. Localization

The stress field  $\sigma^1(x, y)$  is the first term of the asymptotic expansion (8) of the stress field  $\sigma^\epsilon(x)$  solution of the initial exact problem. The field  $\sigma^1(x, y)$  is called the microscopic stress field. If we imagine that at each point  $x \in \Omega$ , there is a small  $\epsilon Y$  period with its composite structure, then  $\sigma^1(x, y)$  gives, for  $x$  kept fixed in  $\Omega$ , a stress field in this period.

It can be shown that  $\sigma^\epsilon(x) - \sigma^1(x, \frac{x}{\epsilon})$  tends to zero in the  $L^1(\Omega)$  norm when  $\epsilon$  tends to zero. This proves that  $\sigma^1(x, \frac{x}{\epsilon})$  is a good approximation of  $\sigma^\epsilon(x)$  when  $\epsilon$  is small. The microscopic stress field  $\sigma^1(x, y)$ ,  $y = \frac{x}{\epsilon}$  can be calculated as follows :

- i) First we obtain the six  $X^{kh}(y)$  vector fields on  $Y$ , each one been associated with tensor  $C^{kh} = C^{hk}$ . These six vector-fields are solution of problem (19), which is an elastic type problem on the inhomogeneous period  $Y$ .
- ii) From the vector fields  $X^{kh}(y)$  we get the homogenized coefficients  $q_{ij}^{kh}$  by formula (22).
- iii) We solve the macroscopic scale, homogenized elastic problem (24) (25) on  $\Omega$ . It gives the macroscopic stress field  $\Sigma(x)$  and the macroscopic strain field  $e_x(u^0) = E(x)$ , for  $x \in \Omega$ .
- iv) Localization procedure : using formula (20) we can calculate  $\sigma^1(x, y)$ . For  $x$  fixed in  $\Omega$ , this stress field on  $Y$  shows how the macroscopic stress  $\Sigma(x) = \langle \sigma^1(x, y) \rangle$  is localized in an  $\epsilon Y$  period at  $x \in \Omega$ .

It can be proved that when  $\epsilon$  tends to zero, the stress field  $\sigma^\epsilon(x)$  tends to  $\Sigma(x)$  in the weak  $L^2(\Omega)$  topology. Nevertheless  $\sigma^1(x, \frac{x}{\epsilon})$  is a better approximation of  $\sigma^\epsilon(x)$  than  $\Sigma(x)$  : the norm  $L^1(\Omega)$  convergence implies that

$$\sigma^\epsilon(x) - \sigma^1(x, \frac{x}{\epsilon})$$

tends to zero for almost every point in  $\Omega$ , while the weak  $L^2(\Omega)$  convergence does not. The macroscopic stress field  $\Sigma(x)$  is just a mean value while  $\sigma^1(x, \frac{x}{\epsilon})$  takes into account the fine periodic structure of the composite material.

### 3 - APPLICATION TO AN ELASTIC MATERIAL REINFORCED BY FIBERS RUNNING IN THE SAME DIRECTION [1] [7]

#### 3.1 - Principle

The computations of the previous paragraph are applied to an elastic material formed from a multitude of resin-impregnated unidirectional fibers whose geometric distribution is periodic in a plane perpendicular to their direction  $x_3$ .

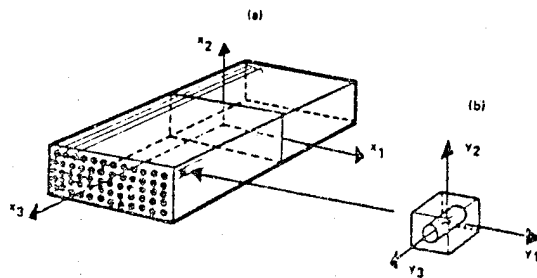


Fig. 8 : a) STRUCTURATION OF FIBERS  
b) BASE PERIOD

Calculation of the homogenized coefficients  $q_{ijkh}$  calls for the resolution of (19). In the present case the coefficients  $a_{ijkh}(y)$  are independent of  $y_3$  ; the result is that the fields  $X^{ij}(y)$  are also independent of  $y_3$  ; in (19) the various indices give a zero contribution when they refer to  $\frac{\partial}{\partial y_3}$  making computation of  $X^{ij}(y)$  a bidimensional problem.

#### 3.2 - Numerical results

In all the cases studied, the homogenized material is orthotropic, in other words the law of behavior has numerous zero elements as shown in the table below :

$$26) \begin{pmatrix} \sigma_{11} \\ \sigma_{22} \\ \sigma_{33} \\ \sigma_{23} \\ \sigma_{13} \\ \sigma_{12} \end{pmatrix} = \begin{bmatrix} q_{1111} & q_{1122} & q_{1133} & 0 & 0 & 0 \\ & q_{2222} & q_{2233} & 0 & 0 & 0 \\ & & q_{3333} & 0 & 0 & 0 \\ & \text{SYM.} & & 2q_{2323} & 0 & 0 \\ & & & & 2q_{1313} & 0 \\ & & & & & 2q_{1212} \end{bmatrix} \times \begin{pmatrix} \epsilon_{11} \\ \epsilon_{22} \\ \epsilon_{33} \\ \epsilon_{23} \\ \epsilon_{13} \\ \epsilon_{12} \end{pmatrix}$$

where  $\{\sigma_{ij}\}$  and  $\{\epsilon_{ij}\}$  are stress and strain tensors.

The law (26) is inverted conventionally to be written [6] :

$$27) \begin{pmatrix} \epsilon_{11} \\ \epsilon_{22} \\ \epsilon_{33} \\ \epsilon_{23} \\ \epsilon_{13} \\ \epsilon_{12} \end{pmatrix} = \begin{bmatrix} \frac{1}{E_1} & -\frac{\nu_{12}}{E_1} & -\frac{\nu_{13}}{E_1} & 0 & 0 & 0 \\ & \frac{1}{E_2} & -\frac{\nu_{23}}{E_2} & 0 & 0 & 0 \\ & & \frac{1}{E_3} & 0 & 0 & 0 \\ & \text{SYM.} & & \frac{1}{2G_{23}} & 0 & 0 \\ & & & & \frac{1}{2G_{13}} & 0 \\ & & & & & \frac{1}{2G_{12}} \end{bmatrix} \begin{pmatrix} \sigma_{11} \\ \sigma_{22} \\ \sigma_{33} \\ \sigma_{23} \\ \sigma_{13} \\ \sigma_{12} \end{pmatrix}$$

bringing out the following :

The Young's moduli  $E_1, E_2, E_3$  in the directions of orthotropy

The Poisson's coefficient  $\nu_{23}, \nu_{13}, \nu_{12}$

The shear moduli  $G_{23}, G_{13}, G_{12}$

The numerical results which follow have been obtained by using the MODULEF code [2]. They have been produced for numerous values of the ratio of impregnation and various forms of the cross section of the fibers.

We give here a part of the results obtained for various forms of fiber, and also the curves showing the change in these coefficients with respect to the ratio of resin impregnation for fibers of circular section (Fig. 9 - 10 - 11).



ALIGNED CIRCULAR FIBER

FIBER

$$\begin{aligned} E_1 &= 3.8 \cdot 10^5 \text{ MPa} & G_{23} &= 2 \cdot 10^4 \text{ MPa} \\ E_2 = E_3 &= .145 \cdot 10^5 & G_{12} = G_{13} &= 3.8 \cdot 10^4 \text{ MPa} \\ \nu_{12} = \nu_{13} &= .22 & \nu_{23} &= .25 \end{aligned}$$

RESIN

$$E = 3520 \text{ MPa} \quad \nu = .38$$

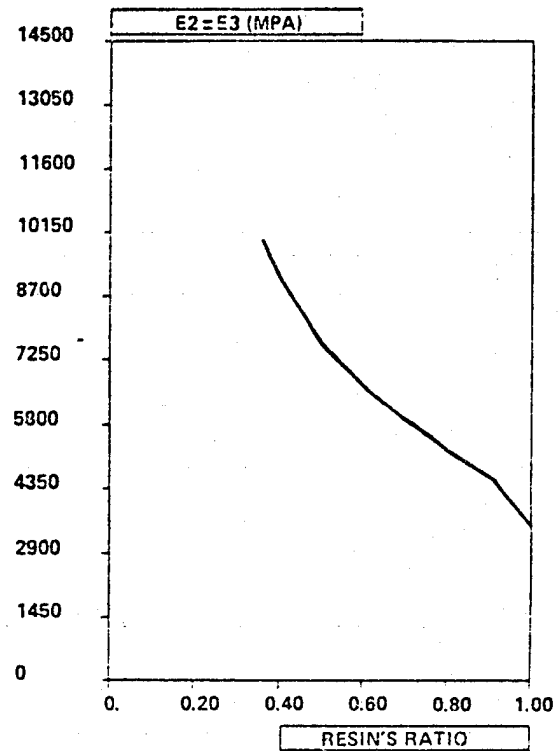
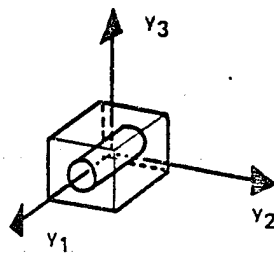


Fig. 10 : VARIATION OF TRANSVERSE YOUNG's MODULI

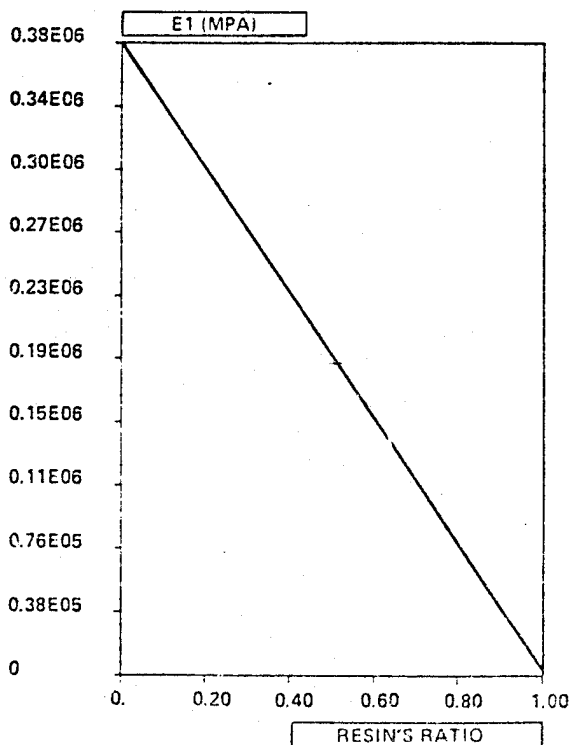


Fig. 9 : VARIATION OF LONGITUDINAL YOUNG's MODULI

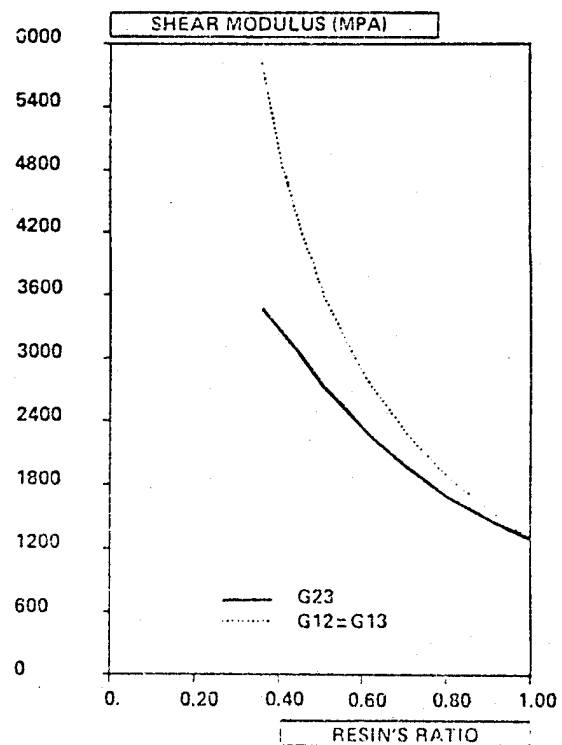


Fig. 11 : VARIATION OF SHEAR MODULI

### 3.3 - Anisotropy curves (Fig. 11)

It is important to note that the homogenized media obtained are generally not transversally isotropic. This comment is clearly demonstrated if the Young's modulus is calculated in transverse direction with polar angle  $\theta$ . By applying the Young's modulus on vector radius we obtain the curves given in Figure 12. For the material to be transversally isotropic, the curves plotted should be arcs of a circle centered at the origin.

Note :

The Young's modulus in direction  $\theta$  is given by :

$$\frac{1}{E(\theta)} = \frac{1}{E_2} \cos^4 \theta + \frac{1}{E_3} \sin^4 \theta + \sin^2 \theta \cos^2 \theta \left( -\frac{2\nu_{23}}{E_2} + \frac{1}{G_{23}} \right)$$

This relation enabled the anisotropy curves in Figure 12 to be plotted.

The material is transversally isotropic if  $E(\theta)$  is not dependent on  $\theta$ , which is equivalent to

$$E_2 = E_3 = 2 G_{23} (1 + \nu_{23})$$

RESIN IMPREGNATION RATIO BY VOLUME 50 %  
(FIBERS // TO X1).

FIBER	RESIN
$E_1 = 380000 \text{ MPa}$ ; $G_{23} = 20000 \text{ MPa}$ ; $\nu_{23} = .25$	$E = 3520 \text{ MPa}$
$E_2 = 14500 \text{ MPa}$ ; $G_{13} = 38000 \text{ MPa}$ ; $\nu_{13} = .22$	
$E_3 = E_2$ ; $G_{12} = G_{13}$ ; $\nu_{12} = \nu_{13}$	$\nu = .38$

	E1	E2	E3	$\nu_{23}$	$\nu_{12}$	$\nu_{13}$	G23	G12	G13
(a)	192000	9730	9070	.33	.28	.30	2452	5597	3334
(b)	191500	8290	8100	.40	.29	.30	2623	4315	3347
(c)	191500	7620	7620	.44	.29	.29	2755	3662	3662

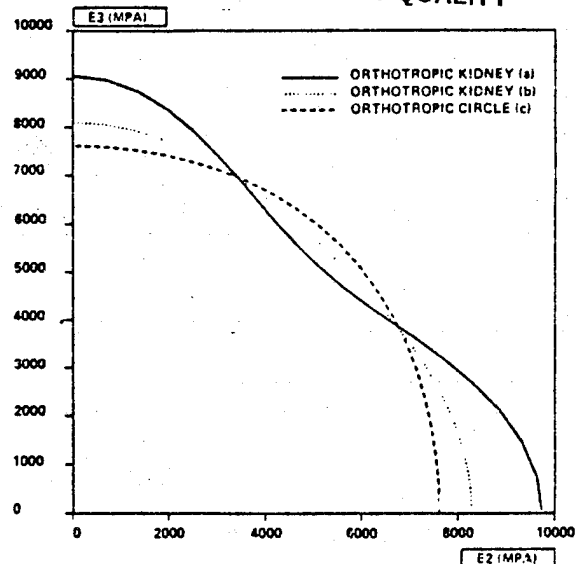


Fig. 12 : TRANSVERSE ANISOTROPY FOR 3 CROSS SECTIONS OF FIBER

### 3.4 - Stagger

If the fibers are staggered, i.e. if a period characterizing the material has the form shown in Figure 13, we obtain diverse characteristics in accordance with the relative values of the sides of lengths of the rectangular cell.

- If  $\lambda = 1$  (square cell) : the characteristics of directions  $Oy_2$  and  $Oy_3$  are identical, and have the same Young's modulus in particular.
- If  $\lambda = \sqrt{3}$ , i.e. if the fibers are located at the apexes of an equilateral triangle (Fig. 13) it can be shown that the material is transversally isotropic. This property is true for any impregnation level of the resin.
- The bisecting directions  $O\tilde{y}_2$  and  $O\tilde{y}_3$  play the same roles irrespective of the values of  $\lambda$  and the impregnation. In particular, the Young's moduli  $\tilde{E}_1$  and  $\tilde{E}_2$  in these directions are always equal.
- In Figure 14 are plotted the Young's and shear moduli corresponding to the various values of  $\lambda$  varying from 1 to 2 and for the same resin impregnation level by volume. For  $\lambda=1$ , the cell is square and naturally  $E_1 = E_2$ . We then find  $E_1 = E_2$  for  $\lambda=\sqrt{3}$  since then the fibers are at the apexes of an equilateral triangle and the material is then transversally isotropic, which implies  $E_1 = E_2$ . In the same figure are plotted the values  $\tilde{E}_1 = \tilde{E}_2$  of the Young's modulus in the bisector directions  $O\tilde{y}_1$  and  $O\tilde{y}_2$ .

For  $\lambda = \sqrt{3}$  we find a triple point since naturally the transverse isotropy then implies

$$E_1 = E_2 = \tilde{E}_1 = \tilde{E}_2$$

# ORIGINAL PAGE 13 OF POOR QUALITY

## CHARACTERISTICS

FIBER : E 84000 MPA

.22

RESIN : E 4000 MPA

.34

RESIN RATIO 36

FIBERS // Y1

REF. 1 : 0 Y1 Y2 Y3

REF. 2 : 0 Y1  $\tilde{Y}_2$   $\tilde{Y}_3$

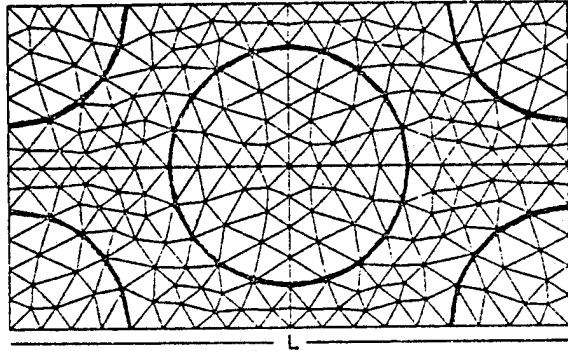
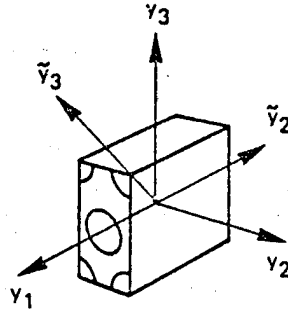


Fig. 13 : EQUIDISTANT STAGGER ( $L=1.73$ )

## 3.5 - Comparison with experiments

The development of this provisional method is aimed at obtaining complete sets of characteristics for three-dimensional computations of composite structures through the finite elements method.

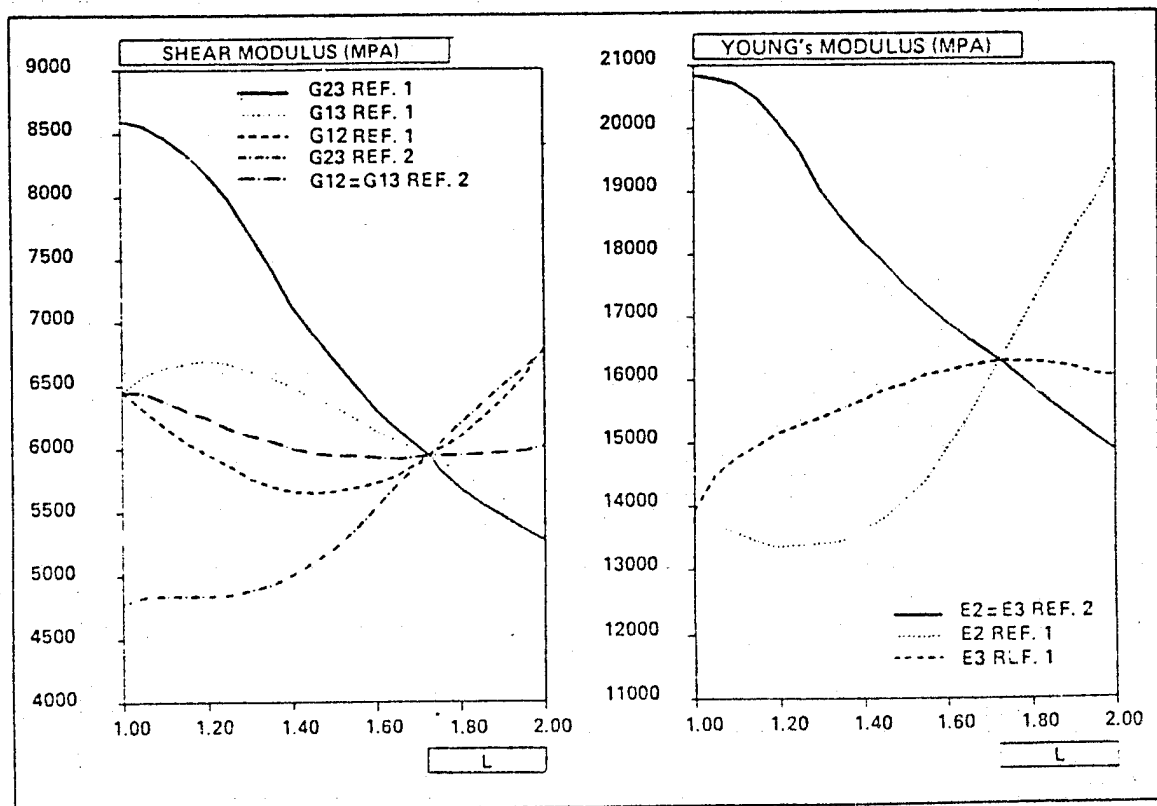
The possibilities of experimental characterization are indeed very reduced. Few tests are reliable, each one being specific to a characteristic, not permitting to reach them all. The results of measurements being very scattered in relation to production batches, mean values have to be used.

The extreme variety of resins give a very wide range of products to be used in production. Each fiber-resin pair can be associated within variable proportions. It is unthinkable to be able to experiment all configurations.

Each material is therefore characterized in an incomplete, dissimilar and inaccurate manner.

Tables presented hereafter explain application of the homogenization theory to the two materials : glass R - Resin Ciba 920 (36 % - Resin in volume) and carbon CTS - Resin Ciba 920 (50 % resin in volume). We have considered several distributions and shapes of fiber.

Taking these values into account, average measured values were assigned to glass-resin composites while values obtained



by transposition of tests results and proportion computation were assigned to carbon-resin composite. As a reminder, characteristics obtained with two bidimensional previsional methods : PUCK [11] and HALPIN-TSAI [14] were also given. For reasons indicated formerly, comparisons must be cautiously made. Results obtained for glass-resin composite with staggered fibers layout at the apexes of an equilateral triangle (ensuring transverse isotropy) are nearest to measured values. With those two methods,  $\nu_{23}$  and  $G_{23}$  cannot be obtained.

As far as carbon based composite is concerned, it is less clear but, in this case, the real shape of the fiber is not observed. On the other hand, when the shape is more accurate («Kidney» shaped), the direction of the fiber does not vary and is therefore as little realistic. Of course, a configuration taking into consideration random direction will probably be nearer to the truth.

For the two considered materials, estimates based on the homogenization theory are nearer to those based on the widely used HALPIN-TSAI method.

The homogenization theory seems efficient to compute the mechanical characteristics of composite materials.

Validity of the results is evidently subjected to the assumptions made on shapes and lay-out of fibers. However, the undeniable advantage of this method aims at supplying complete and consistent sets of values, mutually coherent.

COMPARATIVE TABLE FOR CARBON CTS  
RESIN CIBA 920 (50 % RESIN IN VOLUME) COMPOSITE

	REFERENCE VALUES	HOMOGENIZATION THEORY			OTHER PREVISIONAL METHODS	
		ALIGNED CIRCULAR FIBERS	STAGGERED CIRCULAR FIBERS	"KIDNEY" SHAPED FIBERS (MEAN VALUES)	PUCK	HALPIN-TSAI
$E_1$ (MPa)	120 000	119 299	119 293	119 290	119 260	119 260
$E_2$ (MPa)	6 000	6 284	6 035	8 000	11 620	5 620
$E_3$ (MPa)	6 000	6 284	6 035	7 950	11 620	5 620
$\nu_{12}$	0.28	0.299	0.299	0.31	0.3	0.3
$\nu_{13}$	0.28	0.299	0.299	0.29	0.3	0.3
$\nu_{23}$	0.20	0.435	0.457	0.27	—	—
$G_{12}$ (MPa)	3 800	3 454	3 391	4 500	4 250	3 350
$G_{13}$ (MPa)	3 800	3 454	3 391	3 200	4 250	3 350
$G_{23}$ (MPa)	2 500	2 631	3 266	2 100	—	—

COMPARATIVE TABLE FOR GLASS R-RESIN  
CIBA 920 (36 % RESIN IN VOLUME) COMPOSITE

ORIGINAL PAGE IS  
OF POOR QUALITY

	MEASURED VALUES	HOMOGENIZATION THEORY		OTHER PREVISIONAL METHODS	
		ALIGNMENT CIRCULAR FIBERS	STAGGERED CIRCULAR FIBERS	PUCK	HALPIN-TSAI
E <sub>1</sub> (MPa)	55 000	55 226	55 215	54 450	54 450
E <sub>2</sub> (MPa)	17 000	20 275 ( $\tilde{E}_2 = 13\,496$ )	16 016	18 800	18 570
E <sub>3</sub> (MPa)	17 000	20 275 ( $\tilde{E}_3 = 13\,496$ )	16 016	18 800	18 570
$\nu_{12}$	0.26	0.253	0.256	0.264	0.264
$\nu_{13}$	0.26	0.253	0.256	0.264	0.264
$\nu_{23}$	—	0.229 ( $\tilde{\nu}_{23} = 0.487$ )	0.357	—	—
G <sub>12</sub> (MPa)	5 600	6 383	5 887	6 990	5 560
G <sub>13</sub> (MPa)	5 600	6 383	5 887	6 990	5 560
G <sub>23</sub> (MPa)	—	4 539 ( $\tilde{G}_{23} = 8\,250$ )	5 882	—	—

### 3.6 — Microscopic stress field

Given a structure consisting of a unidirectional material and subjected to a simple shearing overall stress field within the plane (1,2) normal to the direction of fibers, the biaxial stress tensor at macroscopic level is :

$$\begin{bmatrix} 0 & \sigma & 0 \\ \sigma & 0 & 0 \\ 0 & 0 & 0 \end{bmatrix}$$

The localization method allows calculation of both the stress field at microscopic level which, in any point of the material period, is :

$$\begin{bmatrix} \sigma_{11} & \sigma_{12} & 0 \\ \sigma_{12} & \sigma_{22} & 0 \\ 0 & 0 & \sigma_{33} \end{bmatrix}$$

and the stress forces at fibre / matrix interface as represented in Figure 15.

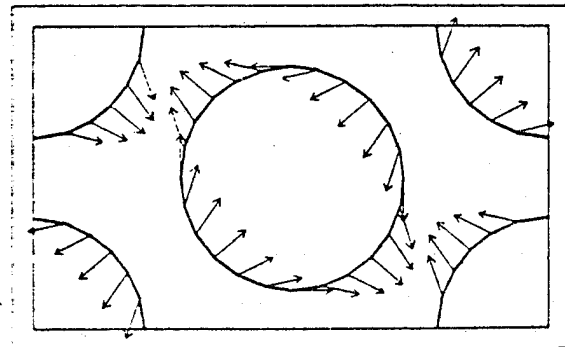


Fig. 15 : STRESS FORCES

#### 4 - APPLICATION TO A PERIODIC STACK OF HOMOGENEOUS LAYERS [4] [7]

##### 4.1 - Principle

We shall consider a periodic stack of a multitude of homogenized layers. Each layer is characterized by a direction of the fibers. In the stack these directions vary periodically whilst remaining orthogonal to axis  $Ox_3$ .

interface:

$$c_{ijkh}(x_3) / \text{layer } (p) = c_{ijkh}^p (\text{constant})$$

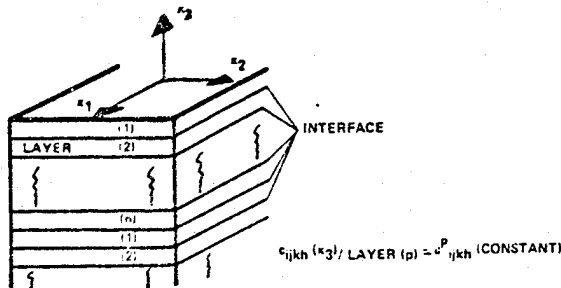


Fig. 16: MULTIPLE LAYERS. EACH LAYER POSSESSES  
A PLANE OF ELASTIC SYMMETRY NORMAL  
TO THE  $x_3$  AXIS (MONOCLINIC SYMMETRY)

In this situation the homogenization formulae are considerably simplified since the problem (19) is then reduced to a system of differential equations which may be solved explicitly. For the details, refer to D. Begis, G. Duvaut, A. Hassim [1] and to the references in this publication.

##### 4.2 - Numerical application

As an illustration we consider two cases :

- 1) a laminate consisting of 3 identical layers disposed periodically. The layers have equal thickness and their fibers orientations are respectively  $-60^\circ$ ,  $0^\circ$ , and  $60^\circ$  with respect to the  $x_1$  - axis. The homogenized material then presents a transverse isotropy which complies with the general results on isotropy, cf. [8] .
- 2) a laminate consisting of 18 layers identical to the above and laid up at successive angles of  $10^\circ$  to each other. It is to be checked that the same result is obtained as in the previous case.

We give in the table presented hereafter the moduli of each layer and the moduli of the composite which are identical for the two cases (3 layers and 18 layers).

	HOMOGENIZED MODULI OF EACH LAYER	HOMOGENIZED MODULI OF COMPOSITE
E1	120 000 MPa	45 128 MPa
E2	6 000 MPa	45 128 MPa
E3	6 000 MPa	6 198 MPa
$\nu_{23}$	0.20	0.188
$\nu_{13}$	0.28	0.188
$\nu_{12}$	0.28	0.30
G23	2 500 MPa	3 015 MPa
G13	3 800 MPa	3 015 MPa
G12	3 800 MPa	17 250 MPa

##### Conclusion

We have presented several applications of the homogenization techniques for computing the coefficients of elasticity of composite materials. Other applications using the localization procedure are contemplated as regards fine analysis of the field of stresses using asymptotic expansions, the effect of defects in the composites [9] and more generally, damage to the materials of composite structure containing inclusions or precipitates.

Strictly speaking, these techniques apply only to absolutely periodic structures, but with the backing of statistical analyses it is possible to identify the fluctuations likely to be produced by periodic defects. It is noted generally that strict periodicity reinforces the anisotropy of the computed homogenized material with respect to the industrial model.

##### BIBLIOGRAPHY

- 1 D. BEGIS, G. DUVAUT, A. HASSIM. Homogénéisation par éléments finis des modules de comportements élastiques de matériaux composites - Rapport de Recherche n° 101, INRIA
- 2 D. BEGIS, A. PERRONNET. Présentation du Club Modulef - INRIA, Mai 1981
- 3 A. BENSOUSSAN, J.L. LIONS, G. PAPANICOLAOU. Asymptotic analysis for periodic structures - NORTH HOLLAND, Publishing Company, 1978
- 4 G. DUVAUT. Matériaux élastiques composites à structure périodique. Homogenization. Theoretical and applied mechanics - W.T. KOITER, ed NORTH-HOLLAND publishing company, 1976
- 5 G. DUVAUT. Effective and homogenized coefficients Symposium on functional analysis and differential equations - LISBOA, Portugal, March 29 - April 2, 1982
- 6 S. FLUGGE. Encyclopedia of Physics. Mechanics of solids II - Springer Verlag, volume 2

- 7 A. HASSIM. Homogénéisation par éléments finis d'un matériau élastique renforcé par des fibres - Thèse de 3ème cycle (TOULOUSE 1980)
- 8 F. LENE, G. DUVAUT. Résultats d'isotropie pour des milieux homogénéisés - CRAS Paris, Tome 293, pp. 477-480 série 2 (Octobre 1981).
- 9 F. LENE, D. LEGUILLON. Etude de l'influence d'un glissement entre les constituants d'un matériau composite sur ses coefficients de comportement effectifs Journal de Mécanique, vol. 20 n° 2, 1981
- 10 F. PISTRE. Calcul des microcontraintes au sein d'un matériau composite
- 11 A. PUCK. Grundlagen der Spnnungs und verformungs Analyse - Dipl. Ing. Kunststoffe. Bd 57. Heft 4 (1967)
- 12 E. SANCHEZ-PALENCIA. Non-Homogeneous media and vibration theory - Lectures Notes in Physics 127, 1980
- 13 P. SUQUET. Une méthode duale en homogénéisation - CRAS Paris, Tome 291 (A), pp. 181-184, 1980
- 14 S.W. TSAI, J.C. HALPIN, N.J. PAGANO. Composite materials Workshop - Technomic Publishing Co. Inc. Connecticut (USA).

**END  
DATE  
FILMED**

**AUG 20 1984**